

Comparison of computational methodologies for ignition of diffusion layers

R. Knikker, A. Dauplain, B. Cuenot and T. Poinso

Centre Européen de Recherche et de Formation Avancée en Calcul Scientifique
42, Avenue Gaspard Coriolis, 31057 Toulouse Cedex, France

Abstract

The prediction of the auto-ignition delay time of fresh fuel in hot air is studied. This problem, encountered in many combustion systems, is in practice often calculated using a simple method, hereafter called *homogeneous mixing ignition* (HMI). This method however neglects transport effects and calculates local instead of global ignition properties. A second method is therefore studied called *linear mixing ignition* (LMI) and consists of the direct simulation of a one-dimensional mixing layer. This method is tested in a hydrogen and methane fuel configuration using detailed and reduced chemistry mechanisms. The results indicate that molecular transport increases the ignition delay, for the methane fuel by about a factor three, but this effect is compensated in the hydrogen case by the small Lewis number of the fuel. Such detailed information is not provided by the HMI method and the LMI approach appears therefore as a minimum requirement for the correct estimation of the ignition delay time.

Keywords: auto-ignition, diffusion layers, computational methods

1 Introduction

The ignition of a fuel stream injected into surrounding hot oxidizer is a problem encountered in many practical situations: for example, multi-staged or sequential combustors and afterburners where fresh fuel is injected at the outlet of the principal combustion chamber and burns in a second chamber, or the so-called lean premixed prevaporized (LPP) burners (Ohkubo et al. 1997) where liquid fuels are atomized by injection into hot air to accelerate the evaporation process (Fig. 1a). In this type of burners, incomplete evaporation and poor mixing may lead to auto-ignition and flame flashback. Auto-ignition is also found in supersonic combustion, for example in scramjets (supersonic ramjets) (Mitani 1995) where the air stream is heated by compression effects. In these devices, the auto-ignition delay time is an important parameter as it effects directly the stand-off distance of the flame from the burner nozzle. Other examples of auto-ignition are found in diesel engines (Kong et al. 1995; Kong et al. 2001; Wan et al. 1997) where the air temperature is increased by compression before fuel injection (Fig. 1b).

This ignition problem may be studied numerically in many different ways. The first and most well-known technique will be called here HMI for homogeneous mixing ignition. Its basis (Fig. 2) is to assume that mixing between the fuel and oxidizer streams is infinitely fast and to parameterize the various mixtures produced by this instantaneous mixing process through the mixture fraction z . A hidden assumption in the HMI approach is that the flow must be ‘equi-diffusive’: all species must diffuse like temperature so that a sample containing z kg of stream 1 and $(1 - z)$ kg of stream 2 has an enthalpy $z h_1 + (1 - z) h_2$ and a mass fraction for species k given by $z Y_{k,1} + (1 - z) Y_{k,2}$, where $Y_{k,1}$ and $Y_{k,2}$ are the mass fractions of species k in streams 1 and 2 respectively. This requires that all species diffuse at the same speed as heat: this is the case when all species Lewis numbers are unity. Each sample of this homogeneous mixing process is isolated from its neighbors and left to

react until ignition. This process can then be easily calculated using a zero-dimensional code such as SENKIN (Lutz et al. 1988) and the ignition time $t_{ign}(z)$ of each sample (characterized by its mixture fraction z) can be measured and plotted as a function of z . This curve usually exhibits a minimum ignition time obtained for a value called the most reacting mixture fraction z_{mr} . It is then often assumed that configurations such as the examples in Fig. 1 will ignite in a time $t_{ign}(z_{mr})$.

The HMI method is obviously a simple and fast method. However, its precision is unclear: assuming that mixing is infinitely fast is a strong simplification. The assumption of an equi-diffusive mixture is also wrong in most practical cases so that the mixture created by the process pictured in Fig. 2 would not lead to the same mass fractions and temperatures in a real mixing phenomenon. Furthermore, the ignition defined in the HMI approach is a *local* ignition which does not necessarily imply *global* ignition of the two streams: if a point ‘ignites’ in a time $t_{ign}(z_{mr})$ but raises its temperature by only 10 or 20 K, it is unclear that the neighboring points will ignite and hence that the global system will ignite. Therefore, two ingredients must be added to this type of ignition studies:

- finite rate diffusion and mixing to incorporate their effects on the ignition delay,
- *global* ignition capabilities, i.e. the propagation of a first ignition spot to neighboring points and to the overall flow.

There are many ways to construct such a simulation and all of them are more complex than HMI. The simplest method is called linear mixing ignition (LMI), since it accounts only for mixing along a line. Mixing is not supposed to be infinitely fast but corresponds to the mixing process observed in the one-dimensional diffusion layer illustrated in Fig. 3. The fuel and oxidizer streams are placed side by side and left to mix and react. This is also the view used in a flamelet approach or in the RIF method (Barths et al. 2002).

The LMI is not often used in practice because it requires the solution of a one-dimensional unsteady problem which is a difficult task when detailed chemical schemes are used. More complex configurations can also be used, for example in DNS of turbulent mixing ignition (Hilbert and Thévenin 2002; Im et al. 1998; Mastorakos et al. 1997). But the LMI is of special interest because of its simplicity and because it satisfies the criteria mentioned above: laminar mixing is accurately predicted, no equi-diffusive assumption is required and global ignition can be studied.

This paper compares HMI and LMI results for hydrogen and methane streams injected into pure hot air. An important question is the accuracy of the HMI method. A second one is the influence of chemical schemes which are an essential parameter in such studies. Section 2 presents the HMI results for hydrogen-air and for methane-air cases. Section 3 then describes the principle of the LMI results, while section 4 compares LMI results to HMI data.

2 Homogeneous ignition calculations (HMI)

The principle of the HMI method is illustrated in Fig. 2. A homogeneous mixture is obtained by adding z kg of fuel to $(1 - z)$ kg of hot air through an infinitely-fast mixing process without chemical reactions. Each mixture is then treated as an isolated sample and left to react up to ignition. Note that this procedure is strictly valid in case of unity Lewis numbers and an approximation to reality since Lewis numbers have different values for each species.

The properties of each homogeneous mixture are uniquely defined by the mixture fraction z . However, for detailed reaction mechanisms containing many different species there is no unique definition of the mixture fraction. We adopt the definition proposed

by Bilger (1988) preserving the stoichiometric value even under differential diffusion and consistent with the mixing procedure of Fig. 2. For hydrogen flames, the mixture fraction is defined as:

$$z = \frac{Y_H/2W_H - (Y_O - Y_{O,air})/W_O}{Y_{H,fuel}/2W_H + Y_{O,air}/W_O} \quad (1)$$

and for methane flames:

$$z = \frac{2Y_C/W_C + Y_H/2W_H - (Y_O - Y_{O,air})/W_O}{2Y_{C,fuel}/W_C + Y_{H,fuel}/2W_H + Y_{O,air}/W_O} \quad (2)$$

where Y_C , Y_H and Y_O are the mass fractions of respectively the carbon, hydrogen and oxygen elements; W_C , W_H and W_O are the corresponding atomic weights and the subscripts *fuel* and *air* refer to the initial conditions in respectively the fuel and air stream. The mixture fraction according to these definitions is a passive scalar normalized to range from $z = 0$ in pure air to $z = 1$ in pure fuel.

The species mass fractions Y_k of each mixture are now given by $Y_k = z Y_{k,fuel} + (1 - z) Y_{k,air}$. Similarly, the enthalpy is calculated from $h = z h_{fuel} + (1 - z) h_{air}$. The temperature of the mixture is obtained from h , Y_k and the pressure p using an iterative Newton method.

The ignition delay of each mixture (characterized by z) is calculated with the SENKIN code (Lutz et al. 1988) using a fixed pressure. For a typical calculation, ignition is characterized by a period of radical build-up without significant heat-release, followed by an exponential increase of the temperature. Although the ignition delay time can be defined in many different ways, it is defined here as the instant of maximum heat release corresponding to the inflection point in the temperature curve.

Hydrogen flame

For the hydrogen case, the conditions of Hilbert and Thévenin (2002) are adopted allowing the comparison of their turbulent ignition results with our calculations. The oxidizer is heated air at a temperature of $T_{air} = 1100$ K composed of 21 % volume of oxygen and 79 % of nitrogen ($X_{O_2,air} = 0.21$ and $X_{N_2,air} = 0.79$). The fuel is hydrogen diluted in nitrogen at a temperature of $T_{fuel} = 300$ K. The hydrogen and nitrogen mole fractions are respectively $X_{H_2,fuel} = 0.25$ and $X_{N_2,fuel} = 0.75$. The pressure is equal to the atmospheric pressure ($p = 1$ atm). The stoichiometric mixture fraction for these conditions is equal to $z_{st} = 0.56$. Contrary to Hilbert and Thévenin (2002), the kinetic reaction mechanism of Yetter et al. (1991) is used here for the hydrogen case. This mechanism has been used successfully in other ignition studies (see for example Im et al. 1998; Kreutz and Law 1996). The results of these HMI calculations are shown in Fig. 4a. The ignition delay is plotted over a wide range of mixture fractions and a clear minimum is found at the mixture fraction $z_{mr} = 0.059$, often called the *most reactive* mixture fraction. The minimum homogeneous ignition delay time is noted $t_{HMI} = t_{ign}(z_{mr})$ and is $t_{HMI} = 0.34$ ms. Note that for mixture fractions around z_{mr} , the ignition delay does not vary significantly as a function of the mixture fraction but remains close to t_{HMI} .

At high values of the mixture fraction, the ignition delay shows an almost exponential behavior: in this regime, the ignition delay depends mainly on the temperature of the mixture which varies almost linearly with z . The slope of the curve can be related to an activation temperature through the empirical relation $t_{ign} \propto \exp(T_{act}/T)$. Using a least-squares method, the activation temperature is estimated at $T_{act} \sim 21,300$ K, which is the order of magnitude of values found in the literature. In Fig. 4a, higher values of the mixture fraction are not plotted as they correspond to extremely long ignition delays.

Methane flame

The conditions of the methane flame are chosen to give a minimum ignition delay time of the same order of magnitude as for the hydrogen flame. The oxidizer is again heated air, although the temperature is increased to $T_{air} = 1400$ K in order to reduce the ignition delay and the computational time. The fuel is a mixture of methane and nitrogen in equal volume fractions ($X_{CH_4} = 0.5$, $X_{N_2} = 0.5$) and a temperature of $T_{fuel} = 300$ K. The pressure is $p = 5$ atm. At these conditions, the stoichiometric mixture fraction is equal to $z_{st} = 0.14$.

Homogeneous ignition delays are calculated using three different reaction mechanisms, see Fig. 4b. The GRI 3.0 mechanism is the most detailed and most recent reaction mechanism and is used here as the reference. The difference with the older version 1.2 is very small though, which justifies the use of this mechanism for this problem. Also plotted are results obtained with the reduced 12-step mechanism proposed by Sung et al. (1998), which has been developed for methane oxidation from the GRI 1.2 mechanism. It fits the original mechanism quite well and offers therefore a considerable reduction of computational costs without losing precision on major chemistry effects. For this reason, this mechanism is retained in the calculations presented below. Finally, the ignition delay results are also compared to the experimental fit (symbols in the figure) proposed by Krishnan and Ravikumar (1981), which reads:

$$t_{ign} = 2.21 \times 10^{-14} \exp(22659/T) [O_2]^{-1.05} [CH_4]^{0.33} \quad (3)$$

where t_{ign} denotes the ignition delay time, T is the temperature and $[O_2]$ and $[CH_4]$ are the molar concentrations (mol/cc) of oxygen and methane. Note that the activation temperature is of the same order of magnitude as for the hydrogen flame. The general agreement of the experimental fit with the numerical results is very good, considering the limited range of operating conditions for which the experiments are conducted. The lean

flame limit $z \rightarrow 0$, for example, is a strong extrapolation of experimental data and might explain the difference at these points with the numerical results.

In contrast to the hydrogen results in Fig. 4a, the exponential regime of the ignition delay for methane continues very far towards the lean side. The curve deviates from this exponential behavior only for very small values of the mixture fraction. Apparently, the temperature dependency on the ignition delay is much stronger than the influence of the methane concentration. The review paper by Spadacinni and Colket III (1994) already pointed out that the ignition delay times of methane mixtures are relatively insensitive to the methane concentration, in particular at very lean conditions. Methane differs at this point from other hydrocarbon fuels, due to the fact that the methyl radical CH_3 , the primary hydrocarbon radical formed from methane, is relatively stable and leads to chain-terminating reactions, rather than chain-branching reactions (Westbrook 2000). Note also in this context the positive exponential factor for the methane concentration in Eq. (3).

Nonetheless, a minimum ignition delay is observed for the numerical results in Fig. 4b. When using the 12-step mechanism, this minimum is located at a mixture fraction of $z_{mr} = 0.002$ and corresponds to an ignition delay time of $t_{HMI} = 0.49$ ms. The local temperature increase during ignition at this most reactive mixture fraction is only 26 K. The term *most reactive* is here clearly not adequate. Note that when pressure is increased, this mixture fraction corresponding to a minimum ignition delay shifts further towards the lean side and eventually disappears altogether. A most reactive mixture fraction does not exist in this case.

As already pointed out, the term ‘ignition’ used in the HMI context is not to be confused with *global* flame ignition. Indeed, an infinitely small concentration of methane, brought to sufficiently elevated temperature, will always react rapidly although the resulting heat release might not be sufficient to ignite a flame globally. The global ignition mechanism

is governed by a balance between fast ignition and sufficient heat release. This point will be further investigated with the one-dimensional LMI calculations in the next section.

3 Laminar mixing ignition calculations (LMI)

The one-dimensional ignition problem illustrated in Fig. 3 is calculated using a direct numerical simulation (DNS) code called NTMIX (Baum 1994), which is coupled to a vectorized version of the CHEMKIN library (Kee et al. 1989). This code has been extensively used in earlier numerical studies including hydrogen and hydrocarbon premixed/diffusion flames. It solves the Navier-Stokes equations and the species equations for detailed chemistry on regular meshes. A sixth order compact finite difference scheme is used to compute first and second order derivatives on interior points, while a compact fourth order scheme is used for the boundary points (Lele 1992). Time advancement is obtained with an explicit third-order Runge-Kutta method using a low storage technique (Wray 1989). Species molecular transport is modeled using Fick's law with diffusion velocities calculated from the binary diffusion coefficients. Dufour and Soret effects (Bird et al. 1960) are taken into account. To ensure species conservation, a correction velocity equal for all species is added to the convection velocity, which in combination with Fick's law corresponds to the best first order approximation of the exact diffusion problem (Giovangigli 1991).

Boundary conditions are calculated using the Navier-Stokes characteristic boundary conditions (NSCBC) formulation (Poinsot and Lele 1992), which has been extended to handle multi-species problems (Baum et al. 1995). The left boundary is entirely non-reflecting, while a small relaxation is applied at the right boundary to avoid drift of the mean pressure in the computational domain. No relaxation is applied to the velocity, but drifting problems are not encountered.

The time step Δt is limited by the classical stability criteria defined by $CFL = c \Delta t / \Delta x < 0.6$ for the convective part and $Fo = \nu \Delta t / \Delta x^2 < 0.1$ for the diffusive part, where Δx is the distance between two grid points, c is the sound speed and ν the kinematic viscosity. It is well known that the CFL imposes a small time step limit, but for the present complex chemistry problems the chemical reaction terms impose an additional and even stricter limitation on the time step. The characteristic time scale of the chemical reactions can be much smaller than the characteristic time scales of the flow, leading to a very stiff system of equations to solve. The explicit scheme applied in this study may then not be efficient and require very small time steps to obtain a stable solution. This appears to be the case in particular when using the complex reaction mechanisms GRI 1.2 and 3.0 for the ignition of methane in hot air. On the other hand, the 12-step reduced mechanism allows much larger time steps, thereby favoring once more the use of this mechanism for the methane ignition problem.

To correctly resolve the discontinuities at the interface between fuel and hot gases, it is necessary to apply some kind of smoothing on the initial conditions. To that purpose, the one-dimensional calculations are initialized with a mixture fraction profile defined by:

$$z = \frac{1}{2} \left[1 + \operatorname{erf}\left(\frac{x - x_0}{d}\right) \right] \quad (4)$$

where d is a measure for the width of the error-function profile and x_0 is its mid-point position. The initial conditions (enthalpy, pressure and species mass fractions) at each grid point are now obtained from the local mixture fraction following the procedure for the homogeneous case. Eq. (4) describes the analytical solution of the diffusion problem for short times in the case of unity Lewis numbers (equal thermal and molecular diffusion) and constant diffusion coefficients. It is also assumed that no reaction takes place during the short initial diffusion phase. To obtain a solution that corresponds as good as possible to the original physical problem, i.e. initially separated fuel and hot air, the parameter d

has to be chosen as small as possible.

Two different cases are again studied with operating conditions corresponding to those used for the HMI calculations. The following discussion of the LMI results will focus on the following aspects: the influence of the initial conditions, the effect of non-unity Lewis numbers and molecular transport and the relation between the first ignition spot and most reactive conditions. The goal is to explain the differences between the hydrogen and methane ignition processes and to compare the LMI and HMI results.

4 LMI Results

The temperature profiles at different time instants of the LMI simulation for hydrogen are illustrated in Fig. 5a. Between $t = 0$ and $t = 0.3$ ms, the major visual process is molecular diffusion which transforms the steep initial profile into a much broader temperature profile. Temperature increase due to chemical reactions start around $t = 0.35$ ms, mainly on the hot lean side of the profile (i.e. for small values of z). This temperature increase activates chemical reactions in neighboring regions and the flame propagates very rapidly towards the rich side, leaving behind a region with reaction products at elevated temperature. The ignition process of the methane flame shown in Fig. 5b is very similar to the hydrogen flame at first sight, but there are some important differences as will be shown in the following analysis.

First, a suitable definition for the ignition delay time for these one-dimensional configurations must be given. A detailed discussion on this subject can be found in Hilbert and Thévenin (2002). As suggested by the authors, it is convenient to work with the total heat release, defined as:

$$\dot{q} = - \int_{-\infty}^{+\infty} \sum h_k \dot{\omega}_k dx \quad (5)$$

where h_k is the enthalpy of species k and $\dot{\omega}_k$ is the reaction rate of species k . A straight extension of the definition of t_{ign} used in the homogeneous calculations is then based on the maximum of the total heat release and reads:

$$\left. \frac{d\dot{q}}{dt} \right|_{t=t_{ign}} = 0 \quad (6)$$

However, as indicated by similar studies and the homogeneous calculations, the flame will first ignite at very lean conditions and then propagate towards richer regions. The heat release is much higher towards the richer side and ignition according to Eq. (6) will be longer due to the finite propagation velocity of the flame front. An alternative definition which is also tested here, giving slightly shorter ignition delays, is given by:

$$\left. \frac{d^2\dot{q}}{dt^2} \right|_{t=t_{ign}} = 0 \quad (7)$$

Fig. 6 shows the temporal evolution of the maximum temperature in the computational domain and the total heat release for the two cases. The time axis is normalized by the minimum homogeneous auto-ignition delay time t_{HMI} for the respective cases. The number of grid points used in both simulations is $N = 500$ and the stiffness parameter of the initial profile is set to $d = 0.02$ mm. As for the homogeneous calculations, a period of radical build-up with negligible heat release is followed by an exponential increase of temperature in the ignition phase. The two symbols in each figure indicate the ignition delays according to Eqs. (6) and (7): the first point (cross) corresponds to the maximum of the heat release time derivative (Eq. 7) and occurs slightly before the second point (circle) corresponding to the maximum of heat release (Eq. 6). The discussion will mainly focus on the ignition delay according to Eq. (7) as it presents a better estimate of the onset of ignition.

Influence of the initial conditions

The influence of the thickness d of the initial mixing layer on the ignition delay time is shown in Fig. 7. All simulations are performed on a $N = 500$ point grid, except for the smallest value of d where $N = 1000$ is used. In fact, the number of grid points N is adapted in order to correctly resolve the initial profiles (d is resolved on about 5 grid points) and at the same time conserving a computational domain large enough to contain the entire ignition process ($N\Delta x > L_{\min}$, where $L_{\min} \sim 0.2$ cm).

As shown by Fig. 7, for both the hydrogen flame (circles) and the methane flame (squares) the ignition delay time tends toward a unique value for decreasing d . For sufficient small values, the influence of the initial conditions are negligible and the unique solution of an initially separated fuel and air ignition problem is recovered. For comparison, ignition delay times defined by both Eqs. (6) and (7) are plotted. As expected, the point of maximum heat release (Eq. 6) occurs slightly after the ignition delay time following definition (7), but both definitions show the same evolution as a function of d .

To investigate the influence on the ignition delay of the unity Lewis number assumption used for the initial condition, the simulations for hydrogen are repeated using an initialization procedure imitating non-unity Lewis numbers effects. The initial enthalpy profile is still described by an error-function with profile width d , but the profile widths for respectively the hydrogen and oxygen mass fraction are now given by $d_{H_2} = d/\sqrt{Le_{H_2}}$ and $d_{O_2} = d/\sqrt{Le_{O_2}}$. The nitrogen mass fraction is calculated from the requirement that the sum of mass fractions must be equal to unity at each grid point. In the following simulations, the hydrogen and oxygen Lewis numbers are set to $Le_{H_2} = 0.35$ and $Le_{O_2} = 1.2$, corresponding roughly to the mean of the values found on respectively the cold and hot side. Results obtained with this initialization procedure are also plotted in Fig. 7. It is observed that the limit of the ignition delay time for small values of d is exactly the same

as for the unity Lewis number initialization. Of course, this simple approach neglects any coupling between the initial profiles of enthalpy and species, but it confirms nonetheless our findings that the final solution is independent of the initial conditions for sufficiently small values of d .

Effect of Lewis numbers and molecular transport

The hydrogen case is particularly interesting since the operating conditions correspond to those used in Hilbert and Thévenin (2002). In this work, LMI simulations are compared to the ignition in homogeneous isotropic turbulence. The turbulent ignition delay was found to be within less than 10 % of the laminar ignition delay and almost insensitive to the turbulent intensity and length scales. They did not however compare their results with homogeneous calculations. As shown by Fig. 6, the LMI delay of the hydrogen case is very close to the minimum value obtained in the HMI calculation. This may suggest that laminar mixing has almost no influence on the ignition delay. If so, the simple HMI calculations are sufficient to provide a very good estimate of the actual ignition delay, even in turbulent conditions. It turns out however that molecular transport plays an important role in this problem and that LMI simulations are still necessary to estimate correctly the ignition delay.

To show this, the LMI simulation for the hydrogen flame is repeated with unity Lewis numbers for all species. As will be shown later in figure 9, the ignition delay is multiplied by a factor seven with respect to the results obtained with detailed transport. This observation shows the importance of including detailed transport in the calculations, as noted by Hilbert and Thévenin (2002), but also the importance of including molecular transport in this complex chemistry ignition problem. This is expected since molecular mixing tends to disperse radicals created at the most reactive zone. Moreover, the location at which the most reactive conditions are found propagates outwards because

the thickness of the mixing layer increases with time. Hence, laminar mixing prohibits the build-up of the radical pool observed in homogeneous calculations, thereby delaying the ignition process. This is illustrated in Fig. 8, which compares HMI and LMI mass fraction evolutions of the H and O radical for the hydrogen flame. The lines in the figure correspond to mass fractions of the HMI calculation in most reactive conditions and the LMI simulation at the location of the first ignition spot. This fixed location is initially far away from the diffusion layer and in order to allow comparison of mass fractions at the location of highest reactivity, propagating outwards as time advances, the LMI results at points of maximum heat release are also indicated in the figure (symbols). In either case, the difference between the HMI and LMI profiles is marked. The concentration of the radicals for LMI is orders of magnitude lower than for HMI, apart from the very start of the mixing process. Radical build-up in the LMI simulation is much slower than for HMI, but increases suddenly in the last period prior to ignition. It is also seen that the first ignition spot, being initially far away from the mixing layer, remains particularly unreactive for a long period of time. It is only in the second part of the ignition delay that this point becomes most reactive and thus coincides with the symbols in the figure.

The effect of the Lewis number of the fuel on the ignition delay is shown in Fig. 9. In these simulations, the fuel Lewis number is kept constant in the computational domain, while other species are described using detailed transport. For Lewis numbers below unity, the fuel diffuses faster than oxygen and heat and is therefore able to reach regions with high concentrations of oxygen at relative high temperature. It is then expected that decreasing the Lewis number of the fuel shortens the ignition delay. This is clearly observed in Fig. 9a for the hydrogen fuel and (although less pronounced) for methane in Fig. 9b. It is interesting to note that in previous ignition studies (Hilbert and Thévenin 2002; Im et al. 1998; Mastorakos et al. 1997), the first ignition spot in turbulent flows

is often located around the mixing layers that are convex towards the fuel side. At these locations, the diffusion of hydrogen towards high temperature regions with abundance of oxygen is promoted, in the same manner as for the non-unity Lewis number effects of premixed propagating flames.

For comparison, the ignition delay times obtained with the detailed transport model and unity Lewis numbers for all species are indicated in the figure by the dashed-dotted and dashed lines respectively. For the hydrogen flame, the variable Lewis number curve intersects the detailed transport ignition delay at about $Le_{H_2} = 0.3$, which is close to the actual value of the hydrogen Lewis number. Furthermore, the curve approaches the unity Lewis number result for $Le_{H_2} = 1$. These observations suggest that the high diffusivity of hydrogen is for a large part responsible for the acceleration of the ignition process, thereby counterbalancing the delay introduced by the overall mixing process. The agreement with the homogeneous ignition delay is more or less a coincidence due to the specific value for the Lewis number. On the other hand, the Lewis number for the methane fuel is close to one. Therefore, the difference between the results obtained with the detailed transport and the unity Lewis numbers in Fig. 9b remains small. In this case, there is no other mechanism to compensate the delay of the ignition process caused by laminar mixing, resulting in a ignition delay almost three times as long as the homogeneous ignition delay. This finding can be important for practical combustion systems where the auto-ignition delay is a crucial parameter in the flame stabilization mechanism.

First ignition spot and most reactive conditions

As mentioned in § 2, the most reactive mixture fraction for methane is close to zero, which differentiates this case from hydrogen or one-step chemistry where generally this minimum is found at much richer conditions. A previous study on laminar and turbulent mixing ignition with one-step chemistry (Mastorakos et al. 1997) suggested that ignition

always occurs at the most reactive mixture fraction, although their turbulent ignition delay times corresponded more closely to the LMI than the HMI results. It is therefore interesting to study the actual relation between the first ignition spot and the most reactive mixture fraction for complex hydrogen and methane chemistry, and its role on the ignition delay.

In order to investigate more closely the first occurrence of ignition, Fig. 10 shows as a function of time the mixture fractions at which a local maximum of the consumption rate of oxygen is observed. It is possible to find more than one maximum at the same time and this is generally the case after ignition has occurred. As evidenced in Fig. 10a for the hydrogen case, the ignited flame splits up in three parts: a lean premixed flame (I) propagating towards the hot air side, a rich premixed flame (III) propagating towards the fuel, and a diffusion flame (II) which installs itself on the stoichiometric mixture fraction line. This situation is very similar to the triple flame structures observed in the stratification of diffusion flames (Domingo and Vervisch 1996; Kioni et al. 1993). The two premixed flames will eventually be extinguished by the lack of either fuel or oxygen. The diffusion flame survives much longer and represents the globally ignited flame in practical burners. The methane flame shown in Fig. 10b shows a similar behavior. Three flame fronts are again identified and the agreement between the mixture fraction of the diffusion flame and the stoichiometric mixture fraction, indicated by the dashed line in the figure, is very good. The mixture fraction of the lean premixed front (I) decreases as the flame propagates towards the hot air side, in regions where methane is still available. On the other hand, the rich premixed front (III) burns the oxygen remaining on the fuel side and propagates towards regions with higher mixture fractions.

For this ignition study, the first part of the plot before flame split-up is more interesting. In the hydrogen case, one single reaction maximum is found with a local mixture fraction

close to the most reactive mixture fraction, indicated by the dashed-dotted line in Fig. 10a. A slight drift of the local mixture fraction is found at the beginning of the calculation, when reaction rates are however negligible. Otherwise, the mixture fraction at maximum heat release is almost constant up to ignition. Although the value of the local mixture fraction does not exactly correspond to z_{mr} , it suggests nonetheless that this point plays an important role in the global ignition of the flame.

The methane case, Fig. 10b, shows a different pattern. The heat release remains very low even after a time period corresponding to the minimum HMI delay. If the ignition mechanism corresponded to that for hydrogen, ignition should start at the most reactive mixture fraction of $z_{mr} = 0.002$. However, due to the low concentrations of methane at this point, chemical reactions are very weak and molecular transport prevents build-up of radical species. Instead, the mixture fraction at the maximum heat release is from the beginning much higher than z_{mr} and increases steadily during the time period before ignition. Apparently, in contrast to the hydrogen flame, the most reactive mixture is not a relevant parameter for ignition of this methane flame.

5 Conclusions

The ignition of fuel in heated air is studied with detailed and reduced chemistry. Two different methods for the calculation of ignition delay times are compared. The first and simplest method is called *homogeneous mixing ignition* (HMI). It assumes infinitely fast mixing between fuel and air and parameterizes each homogeneous mixture with a mixture fraction z . The ignition delay time for each mixture fraction z is easily calculated with readily available numerical tools. The second method is called *linear mixing ignition* (LMI) and consists of direct simulation of a one-dimensional mixing layer. Although this

approach is more complicated, it adds finite mixing to the ignition problem and allows the calculation of global ignition properties.

Two test cases are considered: a hydrogen flame and a methane flame. For both flames, detailed reactions mechanisms that are adequate for these ignition problems can be found in the literature (Smith et al. ; Yetter et al. 1991). Nevertheless, a reduced reaction mechanism (Sung et al. 1998) is preferred for the methane flame to reduce the number of species and the stiffness of the chemical reaction terms. This mechanism is first compared to full schemes to check its accuracy. It is then used for the rest of the study because it allows a considerable reduction of computational time and the use of simple explicit schemes to calculate the LMI problem.

The HMI delay time of the hydrogen flame, plotted as a function of the mixture fraction z , shows a clear minimum at the so-called *most reactive* mixture fraction. For the methane flame, this minimum is less pronounced and located at very low mixture fractions corresponding to extremely lean conditions: the temperature increase during ignition at these conditions is only 26 K. One might expect that in general the most reactive mixture fraction is close to the stoichiometric mixture fraction if both streams have the same temperature and shifts towards the hot side in other cases. Our results contradict this simple picture and shows that the choice of the fuel has an important influence on the most reactive conditions.

The LMI simulation of the hydrogen flame gives ignition delay times close to the HMI delay time. Contrary to what may be concluded from these observations, the mixing process plays an important role in the ignition mechanism. First of all, mixing delays the ignition process because it prohibits radicals to accumulate at the most reactive conditions. Secondly, the higher diffusivity of hydrogen with respect to heat and other species is responsible for an acceleration of the ignition process as it brings the hydrogen to regions

of high temperature and high oxygen concentration. Both mechanisms counterbalance, resulting in HMI and LMI delay time of the same order of magnitude for the hydrogen flame. On the other hand, it is observed that the LMI delay for the methane flame is almost three times longer than the HMI delay. The difference can be explained by two mechanisms: the Lewis number of methane is close to unity hence the ignition accelerating mechanism is absent, and the heat release at the most reactive mixture fraction is too weak to ignite the flame globally and ignition of richer regions takes more time.

In both cases, the LMI simulation gives important information on the ignition properties of mixing layers. While several previous studies using hydrogen fuels have shown that turbulent and laminar ignition delay times are of the same order of magnitude, this study shows that significant differences can be found between homogeneous and laminar calculations. The LMI problem appears (at least for hydrogen flames) as a minimum but sufficient method to estimate ignition delay times in practical devices. Further study may be necessary to evaluate the effect of turbulence for hydrocarbon flames. For hydrogen flames, the LMI method is a relatively simple task compared to more realistic simulations including for example effects of turbulence. For methane or higher hydrocarbon fuels, the additional chemical species and the stiffness of the resulting system of equations can lead to a significant increase of computational costs with respect to HMI calculations. The use of reduced reaction mechanisms and a careful selection of initial conditions is then necessary for LMI. Such an effort may be necessary since this study shows that the HMI calculation, which are commonly used for the evaluation of ignition times, can be very imprecise because they neglect molecular transport effects.

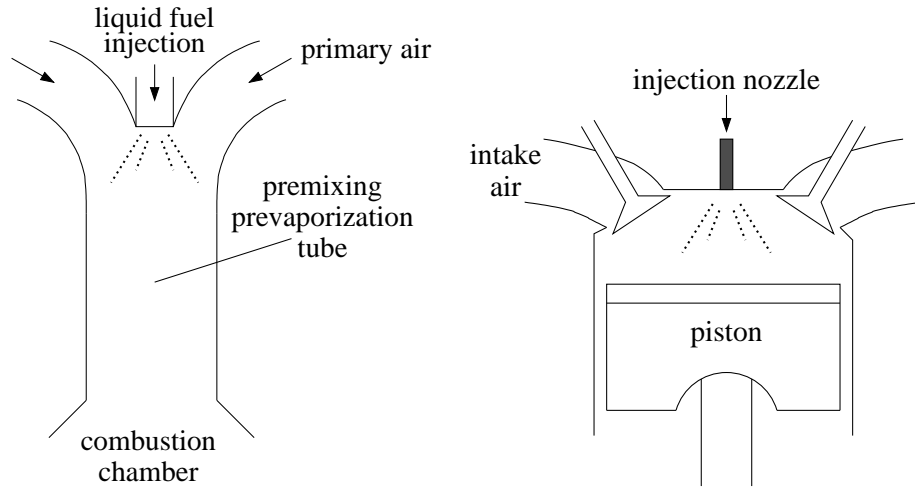
Acknowledgement

The support of ALSTOM Power Switzerland is gratefully acknowledged. Computer time was provided by IDRIS, the supercomputer center of CNRS.

References

- Barths, H., C. Hasse, G. Bikas, and N. Peters (2002). A simulation of combustion in direct injection diesel engines using an eulerian particle flamelet model. *Proc. Combust. Instit.* 28, 1161–1168.
- Baum, M. (1994). *Etude de l'allumage et de la structure des flammes turbulentes*. Ph. D. thesis, Ecole Centrale Paris.
- Baum, M., T. Poinso, and D. Thévenin (1995). Accurate boundary conditions for multicomponent reactive flows. *J. Comput. Phys.* 116, 247–261.
- Bilger, R. (1988). The structure of turbulent premixed flames. *Proc. Combust. Instit.* 22, 475–488.
- Bird, R., W. Stewart, and E. Lightfoot (1960). *Transport Phenomena*. New York: Wiley.
- Domingo, P. and L. Vervisch (1996). Triple flame and partially premixed combustion in auto-ignition of non-premixed turbulent mixtures. *Proc. Combust. Instit.* 26, 233–240.
- Giovangigli, V. (1991). Convergent iterative methods for multicomponent diffusion. *Impact Comput. Sci. Eng.* 3, 244–276.
- Hilbert, R. and D. Thévenin (2002). Autoignition of turbulent non-premixed flames investigated using direct numerical simulation. *Combust. Flame* 128, 22–37.
- Im, H., J. Chen, and C. Law (1998). Ignition of hydrogen-air mixing layer in turbulent flows. *Proc. Combust. Instit.* 27, 1047–1056.
- Kee, R., F. Rupley, and J. Miller (1989). Chemkin II: A fortran package for the analysis of gas-phase chemical kinetics. *Sandia National Laboratories, Rept SAND89-8009B*.
- Kioni, P., B. Rogg, K. Bray, and A. Liñán (1993). Flame spread in laminar mixing layers: the triple flame. *Combust. Flame* 95(3), 276–290.
- Kong, S., Z. Han, and R. Reitz (1995). The development and application of a diesel ignition and combustion model for multidimensional engine simulations. *SAE paper 950278*.
- Kong, S., C. Marriot, R. Reitz, and M. Christensen (2001). Modeling and experiments of hcci engine combustion using detailed chemical kinetics with multidimensional cfd. *SAE paper 2001-01-1026*.
- Kreutz, T. and C. Law (1996). Ignition in non-premixed counterflowing hydrogen versus heated air: computational study with detailed chemistry. *Combust. Flame* 104, 157–175.

- Krishman, K. and R. Ravikumar (1981). *Comb. Sci. Tech.* 24, 239.
- Lele, S. (1992). Compact finite difference schemes with spectral-like solution. *J. Comp. Phys.* 103, 16–42.
- Lutz, A., R. Kee, and J. Miller (1988). SENKIN; A fortran program for predicting homogeneous gas phase chemical kinetics with sensitivity analysis. Technical Report 87-8248, Sandia National Laboratories.
- Mastorakos, E., T. Baritaud, and T. Poinso (1997). Numerical simulation of autoignition in turbulent mixing flows. *Combust. Flame* 109, 198–223.
- Mitani, T. (1995). Ignition problems in scramjets testing. *Combust. Flame* 101, 347–359.
- Ohkubo, Y., Y. Idota, and Y. Nomura (1997). Evaporation characteristics of fuel spray and low emissions in a lean premixed-prevaporization combustor for a 100 kW automotive ceramic gas turbine. *Energy Conversion and Management* 38(10-13), 1297–1309.
- Poinso, T. and S. Lele (1992). Boundary conditions for direct simulation of compressible viscous flows. *J. Comp. Phys.* 101, 104–129.
- Smith, G., D. Golden, M. Frenklach, N. Moriarty, B. Eiteneer, M. Goldenberg, C. Bowman, R. Hanson, S. Song, W. Gardiner Jr., V. Lissianski, and Z. Qin. http://www.me.berkeley.edu/gri_mech.
- Spadacinni, L. and M. Colket III (1994). Ignition delay characteristics of methane fuels. *Prog. Energy Combust. Sci.* 20, 431–460.
- Sung, C., C. Law, and J.-Y. Chen (1998). An augmented reduced mechanism for methane oxidation with comprehensive global parametric validation. *Proc. Combust. Instit.* 27, 295–304.
- Wan, Y., H. Pitsch, and N. Peters (1997). Simulation of autoignition delay and location of fuel sprays under diesel-engine relevant conditions. *SAE paper 971590*.
- Westbrook, C. (2000). Chemical kinetics of hydrocarbon ignition in practical combustion systems. *Proc. Combust. Instit.* 28, 1563–1577.
- Wray, A. (1989). Minimal storage time advanced schemes for spectral methods. Technical report, NASA Ames Research Center, M.S. 202 A-1, Moffet Field, CA94035.
- Yetter, R., F. Dryer, and H. Rabitz (1991). A comprehensive reaction mechanism for carbon monoxide/hydrogen/oxygen kinetics. *Combust. Sci. and Tech.* 79, 97–128.



(a)

(b)

Figure 1: Practical examples involving the ignition of diffusion layers between fuel and hot air. In the LPP concept (a), the liquid fuel is injected into hot air: it vaporizes and mixes with the air stream. During this process, the diffusion layers between air and fuel must not auto-ignite. In diesel engines (b), the liquid fuel is injected into compressed hot air: it vaporizes, mixes with hot air in a diffusion layer and auto-ignites.

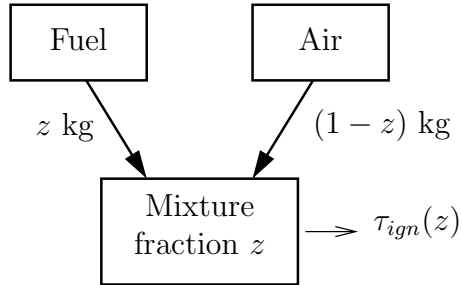


Figure 2: Principle of the homogeneous mixing ignition (HMI) problem.

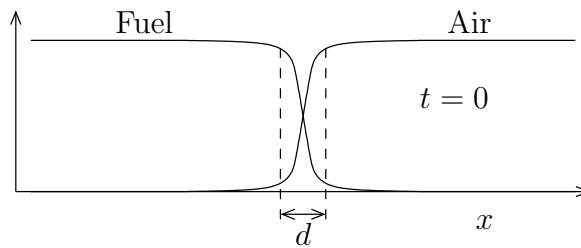


Figure 3: Schematic diagram of the initial condition for the linear mixing ignition (LMI) problem.

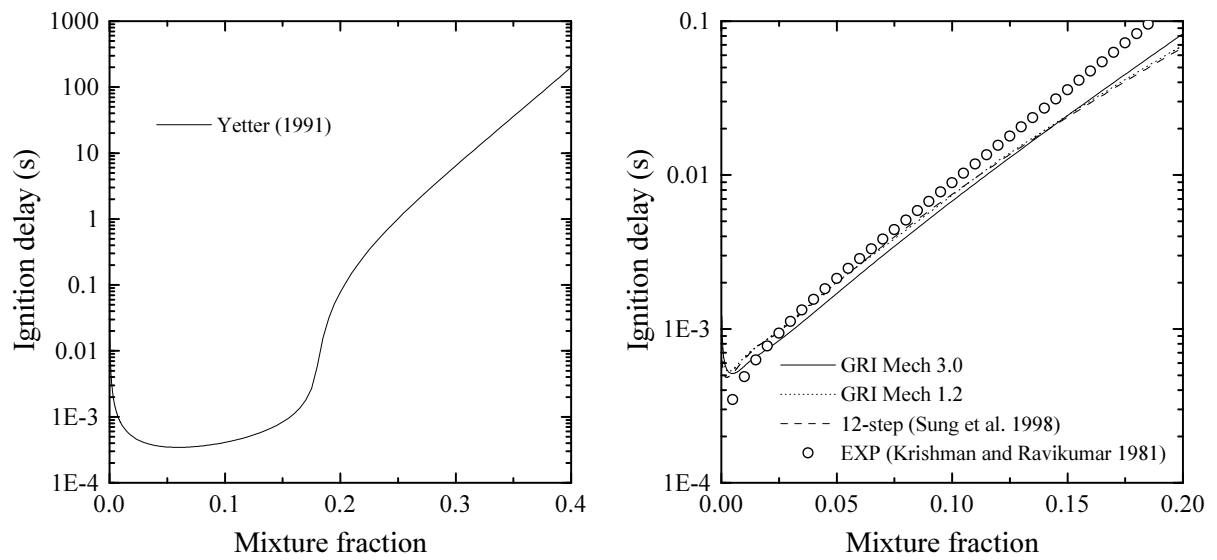
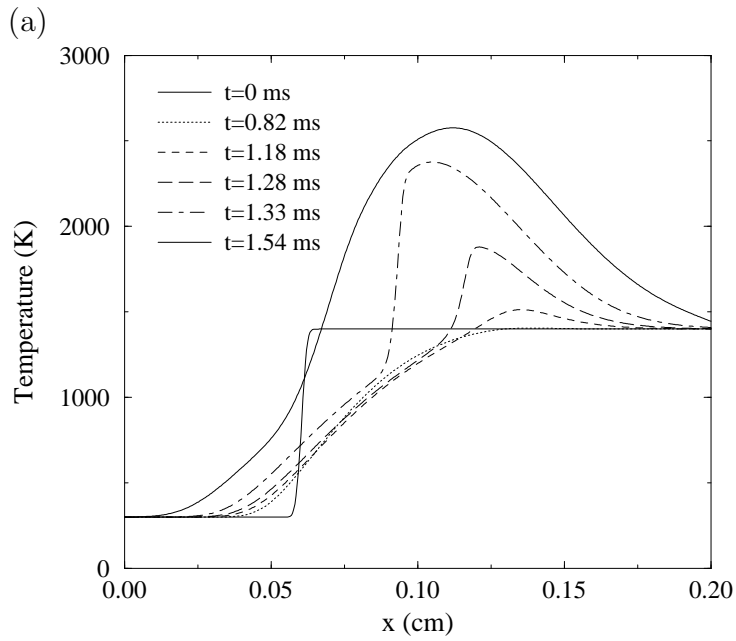
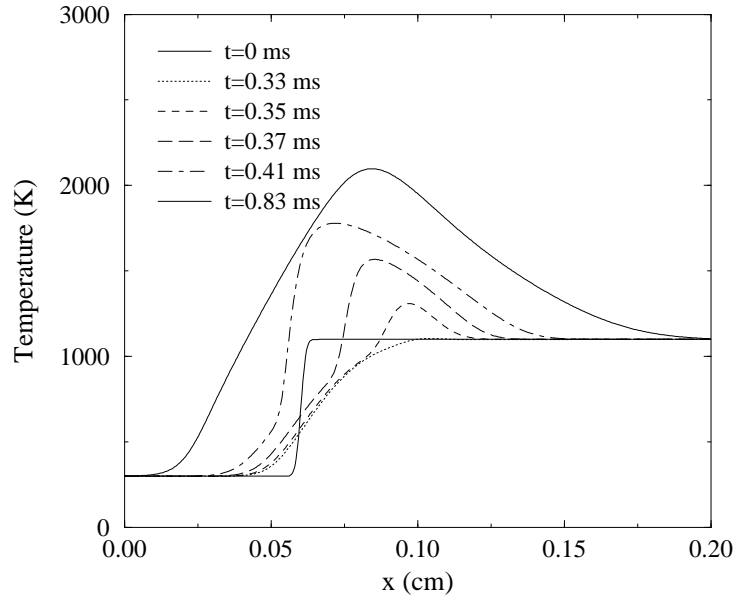


Figure 4: Homogeneous ignition delay plotted as a function of the mixture fraction. (a) $\text{H}_2/\text{N}_2\text{-Air}$, $T_{air} = 1100 \text{ K}$, $T_{fuel} = 300 \text{ K}$, $p = 1 \text{ atm}$, (b) $\text{CH}_4/\text{N}_2\text{-Air}$, $T_{air} = 1300 \text{ K}$, $T_{fuel} = 300 \text{ K}$, $p = 5 \text{ atm}$.



(b)

Figure 5: Temperature profiles at different time instants for (a) the hydrogen flame and (b) the methane flame. For comparison, the ignition delay time according to definition (7) is $\tau_{ign} = 0.34$ ms for the hydrogen flame and $\tau_{ign} = 0.48$ ms for the methane flame.

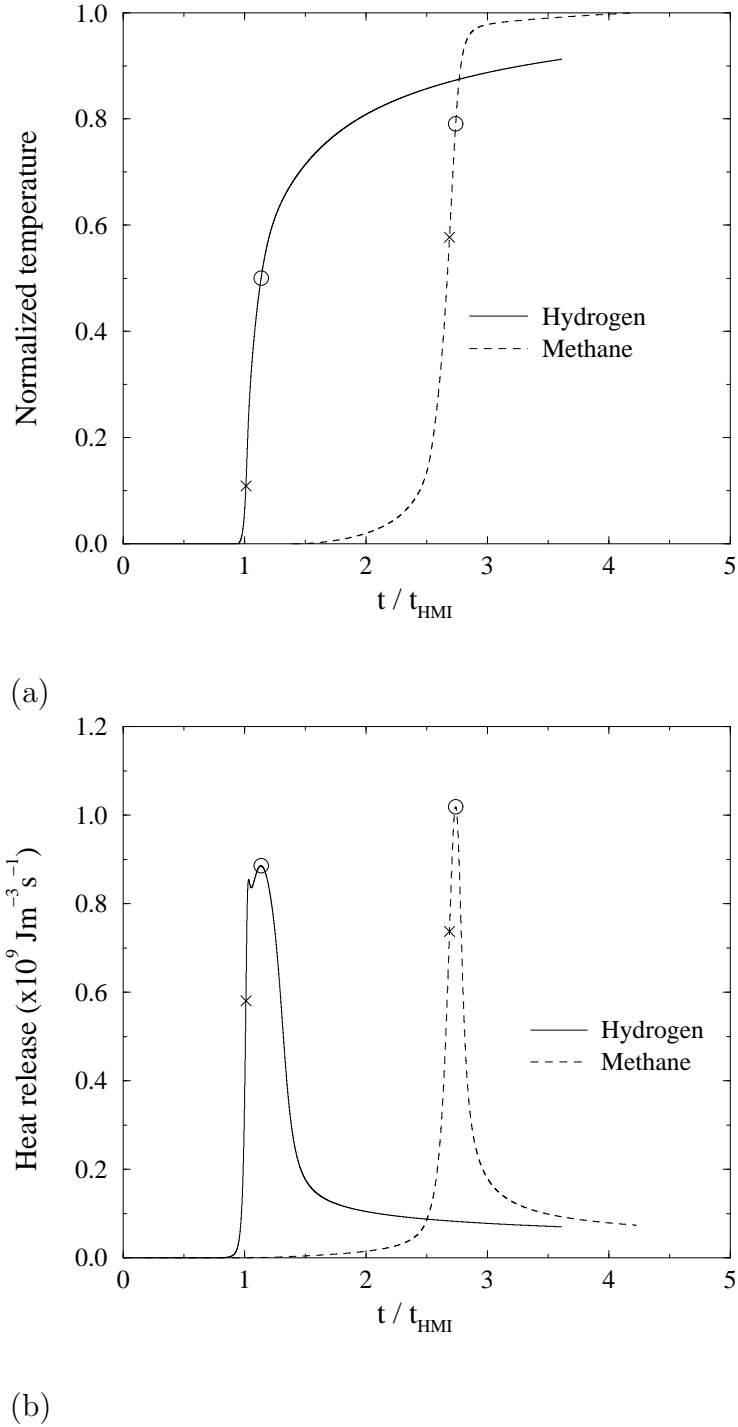


Figure 6: Temporal evolution of the maximum temperature in the computational domain (a) and the total heat release (b) during auto-ignition. The temperature is normalized by the maximum value before and after ignition, the time is normalized by the minimum homogeneous ignition (HMI) delay time for respectively the hydrogen and methane case. The symbols indicate the ignition times according to definitions (7: cross) and (6: circle).

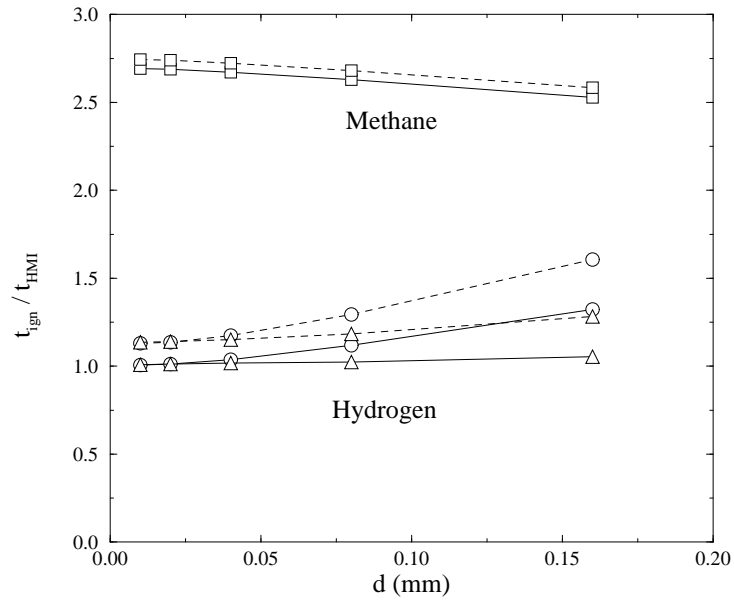


Figure 7: Laminar ignition delay times plotted as a function of the width d of the initial mixing layer. Solid and dashed lines correspond to ignition delays according to definitions (7) and (6). The hydrogen cases are indicated by circles and triangles, the latter corresponding to the non-unity Lewis number initialization, and the methane cases by squares.

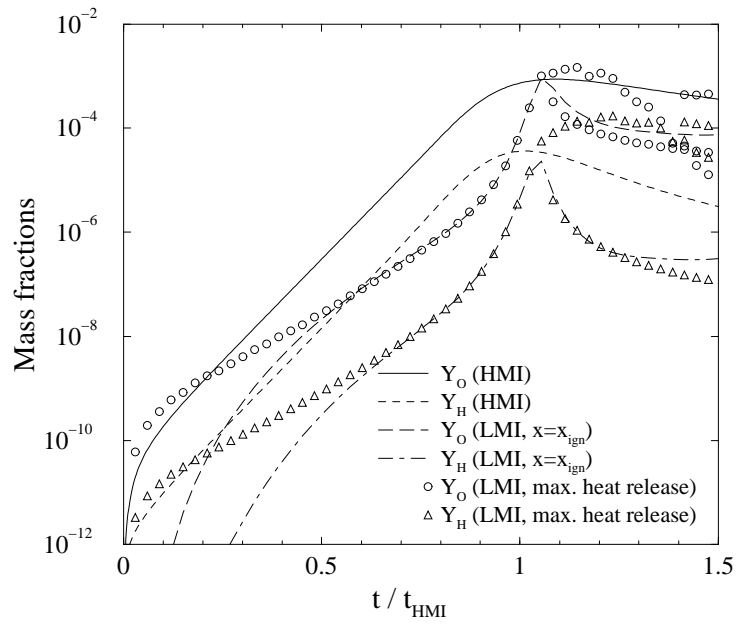


Figure 8: Temporal evolution of the concentration of the radicals O and H for the H_2/N_2 -air simulations. The lines correspond to mass fractions of the HMI simulation and LMI mass fractions at the (fixed) location of first ignition. Symbols indicate LMI mass fractions at locations of maxima in the instantaneous heat release profile.

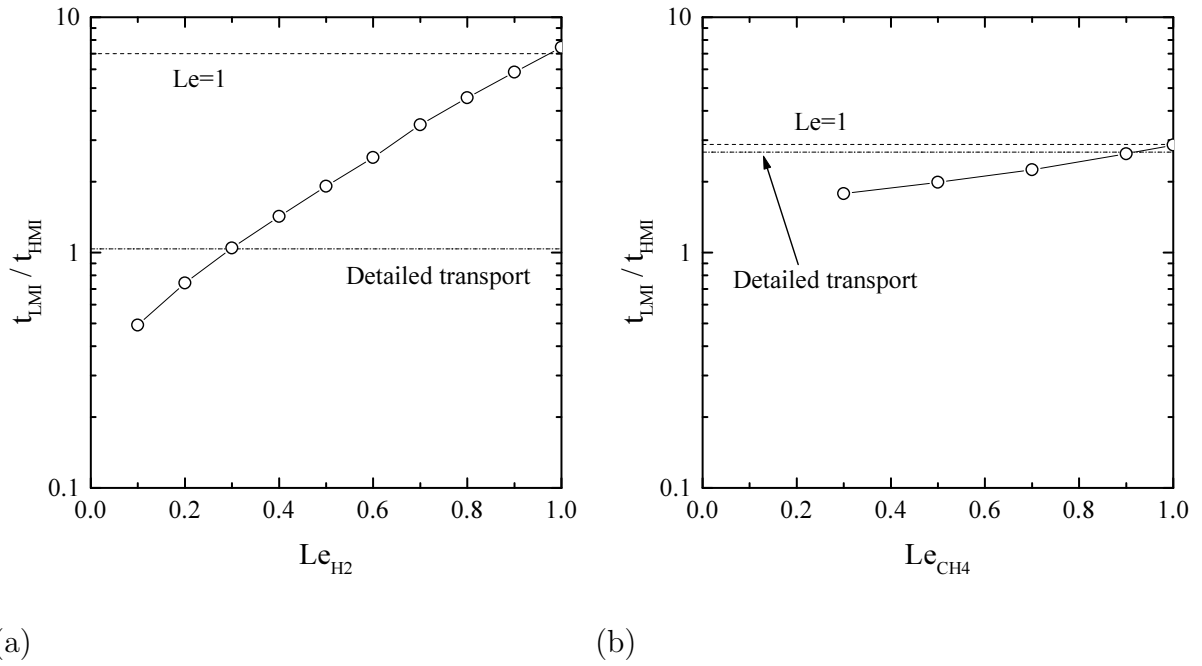


Figure 9: Influence of the Lewis number of the fuel species on the LMI results for (a) the hydrogen flame and (b) the methane flame. Remaining species are described by detailed diffusion. As a reference, dashed lines indicate the ignition delay for detailed diffusion; dot-dashed lines correspond to unity Lewis numbers for all species.

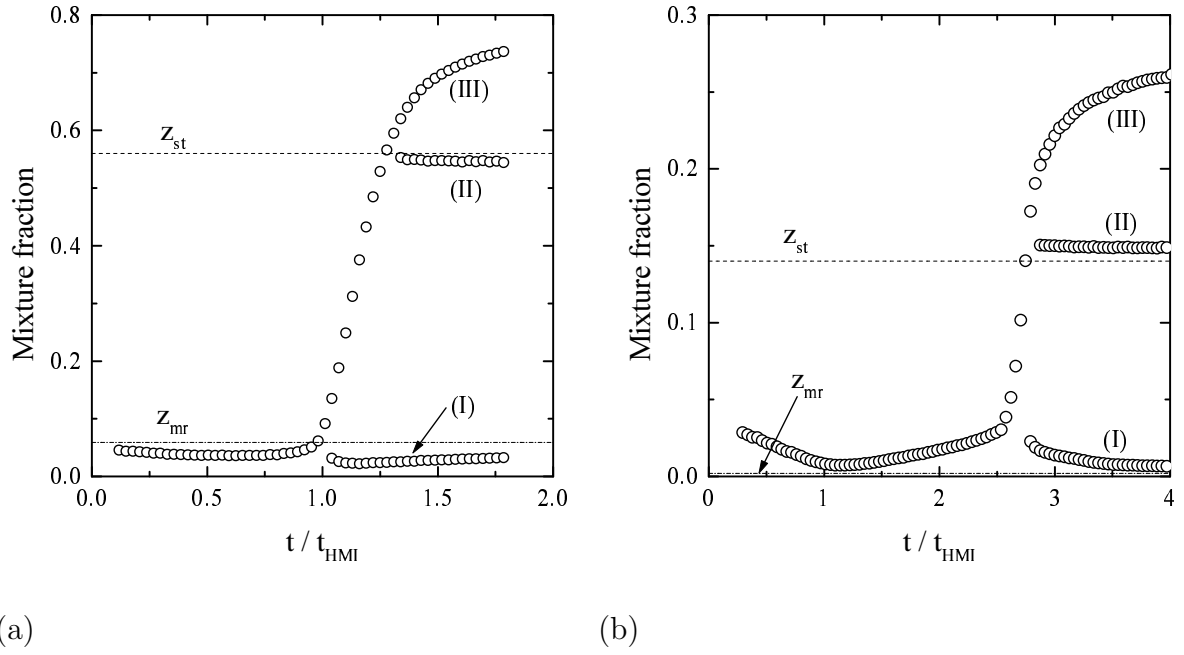


Figure 10: Mixture fraction at local maxima of the consumption rate of oxygen. Results are plotted for the hydrogen case (a) and the methane case (b) as a function of the time, normalized by the respective ignition delay times according to definition (6). Horizontal lines correspond to levels of stoichiometric and most reactive mixture fraction z_{st} and z_{mr} . Roman numbers refer to respectively the lean premixed flame front, the diffusion flame and the rich premixed flame front appearing after ignition.